

Original Article

Three-dimensional reconstruction of coronary arteries based on the integration of intravascular ultrasound and conventional angiography

Cristiano Guedes Bezerra^{a,b}, Gonzalo Daniel Maso Talou^{c,d}, Carlos Alberto Bulant^{c,d}, Breno de Alencar Araripe Falcão^{a,b}, José Mariani Jr.^{a,b}, Pablo Javier Blanco^{c,d}, Raúl Antonino Feijóo^{c,d}, Pedro Alves Lemos Neto^{a,b,*}

^a Instituto do Coração, Hospital das Clínicas, Faculdade de Medicina, Universidade de São Paulo, São Paulo, SP, Brazil

^b Hospital Sírio-Libanês, São Paulo, SP, Brazil

^c Laboratório Nacional de Computação Científica, Ministério da Ciência, Tecnologia e Inovação, Petrópolis, RJ, Brazil

^d Instituto Nacional de Ciências e Tecnologia em Medicina Assistida por Computação Científica, Petrópolis, RJ, Brazil

ARTICLE INFO

Article history:

Received 16 January 2015

Accepted 15 April 2015

Keywords:

Interventional ultrasonography

Angiography

Three-dimensional imaging

Atherosclerosis.

ABSTRACT

Background: Coronary three-dimensional reconstruction with the combination of intravascular ultrasound and angiography offers advantages over computed tomography angiography of coronary arteries. The authors aimed to present the pilot phase of the validation of a new model of three-dimensional reconstruction of coronary arteries.

Methods: This study used angiography and intravascular ultrasound examinations already performed by clinical indication in individuals with known or suspected stable coronary artery disease. Image processing, segmentation, and three-dimensional reconstruction were conducted following specific methodology. For geometrical characterization purposes, tridimensional center lines were obtained.

Results: Three vessels were reconstructed: two left anterior descending arteries and one left circumflex artery. The vessel lumen volume and the overall plaque burden could be easily viewed with three-dimensional reconstruction. The geometric characterization revealed increased absolute values of length, tortuosity, curvature, and torsion, featuring a greater complexity of the center line of the diseased lumen relative to the center line of the external elastic membrane.

Conclusions: This new methodology, which integrates conventional angiography and intravascular ultrasound, has increased the practicality of the reconstructions, with a gain in volumetric accuracy of the vessel and overall visualization of key aspects of atherosclerotic disease, such as plaque remodeling and distribution.

© 2015 Sociedade Brasileira de Hemodinâmica e Cardiologia Intervencionista. Published by Elsevier Editora Ltda. This is an open access article under the CC BY-NC-ND license (<http://creativecommons.org/licenses/by-nc-nd/4.0/>).

Reconstrução tridimensional de artérias coronárias a partir da integração do ultrassom intracoronário e da angiografia convencional

RESUMO

Introdução: A reconstrução tridimensional coronária com a combinação do ultrassom intracoronário e da angiografia apresenta vantagens em relação à angiotomografia de coronárias. Objetivamos apresentar a fase piloto de validação de um novo modelo de reconstrução tridimensional de artérias coronárias.

Métodos: Foram utilizados exames de angiografia e ultrassom intracoronário já realizados por indicação clínica em indivíduos com suspeita ou diagnóstico de doença arterial coronária estável. O processamento das imagens, a segmentação e a reconstrução tridimensional foram realizados seguindo metodologia específica. Para fins de caracterização geométrica, foram obtidas as linhas de centro tridimensionais.

Resultados: Foram reconstruídos três vasos, sendo duas artérias descendentes anteriores e uma artéria circunflexa. O volume da luz do vaso e a carga de placa global puderam ser visualizados com facilidade com a reconstrução tridimensional. A caracterização geométrica revelou aumento dos valores absolutos do comprimento, tortuosidade, curvatura e torção, caracterizando uma maior complexidade da linha de centro da luz doente, em relação à linha de centro da membrana elástica externa.

Palavras-chave:

Ultrassonografia de intervenção

Angiografia

Imagem tridimensional

Aterosclerose

DOI of original article: <http://dx.doi.org/10.1016/j.rbc.2015.12.013>

* Corresponding author: Avenida Dr. Enéas de Carvalho Aguiar, 44, bloco I, 3º andar, Hemodinâmica, Cerqueira César, CEP: 05403-000, São Paulo, SP, Brasil.

E-mail: pedro.lemos@incor.usp.br (P.A. Lemos Neto).

Peer Review under the responsibility of Sociedade Brasileira de Hemodinâmica e Cardiologia Intervencionista.

Conclusões: Essa nova metodologia, que integrou angiografia convencional e ultrassom intracoronário, aumentou a praticidade das reconstruções, com ganho em acurácia volumétrica do vaso e visualização global de aspectos-chave da doença aterosclerótica, como remodelamento e distribuição da placa.

© 2015 Sociedade Brasileira de Hemodinâmica e Cardiologia Intervencionista. Publicado por Elsevier Editora Ltda. Este é um artigo Open Access sob a licença de CC BY-NC-ND (<http://creativecommons.org/licenses/by-nc-nd/4.0/>).

Introduction

Some studies use biplane angiography (AX) for three-dimensional reconstruction of the coronary artery lumen.^{1,2} However, AX is limited to defining the vessel lumen. Intravascular ultrasound (IVUS) is an accurate intravascular imaging technique for plaque quantification and location, since it allows for an accurate assessment from the adventitia to the intima. The combined use of IVUS and AX offers an interesting alternative for coronary three-dimensional reconstruction, outperforming coronary angiography (CT) in terms of accuracy. The ability to reconstruct the entire three-dimensional arterial wall allows for exploitation of the spatial characteristics of plaque. It can also be used for extracting geometrical features for studying the development and progression of atherosclerotic plaques, and for computational fluid dynamics models assessing the hemodynamics repercussions of the plaque.³

This study aimed to present the pilot phase of validation of a new three-dimensional reconstruction model.

Methods

Acquisition of images

For the development of this method, AX and IVUS, performed by clinical indication in patients with known or suspected stable coronary artery disease, from two institutions, the Hospital Sírio-Libanês and the Instituto do Coração, Hospital das Clínicas, University of São Paulo Medical School (FMUSP), both located in the city of São Paulo, SP, Brazil. After compilation, the anonymized data were analyzed by the research team in association with the Laboratório Nacional de Computação Científica (LNCC), where they were processed and integrated. The research project that incorporates this manuscript was approved by the Research Ethics Committee of Hospital Sírio-Libanês and of Hospital das Clínicas (FMUSP).

Reconstructions resulting from IVUS-AX were reprocessed, and geometric shapes of the lumen and the external elastic membrane (EEM) were extracted. Subsequently, the center lines and corresponding volumes of the lumen and the plaque were estimated. Finally, a set of geometric descriptors, calculated from the center line, were used to characterize the geometric shapes of the lumen and the EEM, and the difference between center lines was attributed to the presence of atherosclerotic plaque.

For the acquisition of IVUS images, the iLabTM system was used (Boston Scientific Corporation, Natick, USA), which allowed for the acquisition grayscale-scanned ultrasound images. The intracoronary ultrasound catheter AtlantisSM SR Pro was used (Boston Scientific Corporation, Natick, USA), consisting of a mechanical ultrasound catheter with a frequency of 40 MHz. Automatic IVUS catheter pullbacks were performed in the catheter sheath at the rate of 0.5 mm/s, beginning in the mid-distal third towards the artery ostium, with sectional tomographic image acquisition at a rate of 30 frames/sec.

The movement of the IVUS catheter and vessel curvature hampered the volumetric estimation of plaque burden. The move-

ment of the catheter was corrected using only frames acquired in the diastolic phase of the cardiac cycle.⁴ However, the incorporation of vessel curvature required a location within the catheter space in order to estimate the correct position of the frames in cross-sectional images. Therefore, before the pullback, orthogonal AX was performed in the left anterior oblique and right anterior oblique projections, with cranial and caudal angulation, to estimate the catheter and the sheath spatial location.

Preprocessing and segmentation

To correct the catheter movement due to heartbeat, the frames associated with end-diastolic phase of the cardiac cycle were selected. The mathematical details were provided in a previous publication of this group.⁵ The choice of the end-diastolic phase was due to the minor displacement of the catheter, ensuring a more accurate spatial location during catheter pullback.

The study with IVUS provides a low signal-to-noise ratio (SNR), making vessel lumen and EEM recognition and, in turn, that of plaque burden, difficult. To reduce noise and preserve the structures of interest, an anisotropic diffusion method was employed.⁶

The vessel geometry extraction (segmentation) was performed using an adapted method of active contours.⁷ The energy functions used specifically in the process of minimization of active contours to extract the contour of the vessel lumen and EEM were, respectively,

$$\begin{aligned} \mathcal{E}_{\text{lumen}} &= \frac{1}{2} \int_0^1 \left(\alpha \frac{d\mathbf{v}^\ell}{ds} + \beta \frac{d^2\mathbf{v}^\ell}{ds^2} + \kappa \mathbf{F}_{\text{GVF}} \mathbf{v}^\ell + \kappa_p \mathbf{n} \mathbf{v}^\ell + \eta \gamma e^{-\frac{\|\mathbf{v}^\ell - \mathbf{v}^e\|^2}{\gamma}} \right) ds \\ \mathcal{E}_{\text{EEM}} &= \frac{1}{2} \int_0^1 \left(\alpha \frac{d\mathbf{v}^e}{ds} + \beta \frac{d^2\mathbf{v}^e}{ds^2} + \kappa \mathbf{F}_{\text{GVF}} \mathbf{v}^e + \kappa_p \mathbf{n} \mathbf{v}^e \right) ds \end{aligned}$$

the variables of these equations are described in articles by Maso Talou,⁷ Kass et al.,⁸ and Xu and Prince.⁹

To begin the process of segmentation, manual initialization of the contours was made in the first frame of the sequence of end-diastolic phases of IVUS. Subsequent frames took into account the contours of the previous frame to initialize the method. In case of a failed frame contour or if not sufficiently accurate, the operator redefined the required contours in that frame and continued the segmentation process.

Three-dimensional reconstruction

The orthogonal AX allowed optimal viewing of the catheter and of bifurcations. Observing the cardiac cycle, two frames of AX in diastolic phase were drawn: one with and the other without contrast. The lack of contrast allowed for a full visualization of the IVUS catheter. In addition to these conditions, the IVUS catheter sheath was segmented from the aortic sinus until the end of the transducer, with a biplane snake strategy.¹⁰ During snake initialization, the operator indicated only two points in AX: the location of the transducer and the aortic sinus, generating a straight line between these points. Then, the functional power of snake was optimized to get the segmentation of the catheter as a parametric curve $c(s)$, $s \in [0,1]$.

The next step was to locate the contours of light (SiL) and EEM (SiE) along the trajectory of the catheter $c(s)$. Using the acquisition time of each frame at the end of the diastolic phase of the cardiac cycle (t_i), the position of each frame on the trajectory of the catheter was defined as:

$$s_i = \frac{t_i v_{pb}}{F_{max}}$$

where v_{pb} is the speed of automatic pullback and F_{max} is the number of frames along the whole trajectory. The contour was displayed in the perpendicular plane for T , according to Frenet-Serret formula described to $c(s)$.⁷

$$T = \frac{dc}{ds} / \left\| \frac{dc}{ds} \right\|$$

Finally, the rotation about the axis defined by $c(s)$ was applied, $R(\theta)$, so that the encounter between the contours of IVUS and of the vessel lumen obtained by the contrasted projections of AX was increased. The θ_0 angle, which maximized this encounter, was computed as follows:

$$\theta_0 = \arg \min_{\theta \in [0, 360] \subset \mathbb{Z}} |A_R - A_{AX}|$$

where A_R and A_{AX} were the shadow of the projected lumen by the vascular geometry rebuilt and the vessel lumen by AX, respectively.

Geometric characterization

The three-dimensional reconstruction process provided the spatial configuration of the lumen and EEM (surface meshes) for each heartbeat time. Using ECG synchronization, the surfaces associated with the frames in the end-diastolic phase of the cardiac cycle were extracted.⁵ At this point, for each patient, there were two surface meshes to be characterized, one associated with the lumen and the other with EEM.

Both surfaces could be represented by their center lines,¹¹ which are three-dimensional polylines representing the path taken by the artery, with punctual information of the radius. Next, all center lines were characterized using classical descriptors, such as bending and twisting along the polyline. The centerlines of the arteries were used extensively to characterize the vessels' geometry.¹¹⁻¹⁴

Results

Fig. 1 depicts the three-dimensional reconstruction of three vessels, the first two corresponding to the left anterior descending artery (LAD), and the third to the left circumflex artery (LCx). Table 1 shows the anatomical and geometric descriptors used in this study.

Each case was filtered using the Oriented Speckle Reducing Anisotropic Diffusion (OSRAD), in order to reduce the noise (typical speckles in IVUS images), while preserving the vessel contours. The following parameters were established: $\sigma = 0.7$, $\delta = 20$, $c_{max} = 0.1$, and $c_{min} = 0.5$ for 40 repetitions. Then the IVUS segmentation process was developed, setting the parameters at $\alpha = 1 \times 10^{-4}$; $\beta = 2$; $\kappa = 2$; $\kappa\rho = 0.1$; $\eta = 1.5$; and $\gamma = 15$, for vessel lumen, and $\alpha = 1 \times 10^{-4}$; $\beta = 160$; $\kappa = 1$; and $\kappa\rho = 0$, for EEM segmentation.

The presence of stenosis resulted in disagreement between center lines of the vessel lumen and EEM (asymmetry). The volume of the vessel lumen and the overall plaque burden were obtained by three-dimensional reconstruction. Assuming little remodeling in healthy vessels, the EEM area was almost equal to that of vessel lumen. Thus, comparison of EEM with lumen characteristics provided a broad spectrum of atherosclerotic disease in the vessel in question. Table 1 shows the increased complexity of the center line of the unhealthy lumen relative to the center line of EEM (e.g., increases in

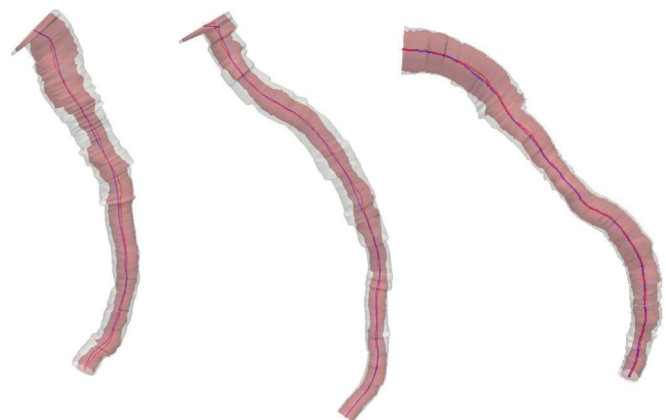


Figure 1. From left to right, three-dimensional reconstruction of left anterior descending artery (cases 1 and 2) and left circumflex artery (case 3). The lumen and the external elastic membrane are represented by red and blue center lines, and by pink and white volumetric filling, respectively.

Table 1 Geometric and anatomical descriptors. The variables in these equations are described in the studies by Bogunović et al.,¹² Mut et al.,¹³ and Meng et al.¹⁴

| Geometric characteristics | Case 1: left anterior descending | | Case 2: left anterior descending | | Case 3: left circumflex | |
|--|----------------------------------|--------------|----------------------------------|--------------|-------------------------|--------------|
| Number of branches | 3 | | 6 | | 2 | |
| Lumen volume, mm ³ | 333.23 | | 381.6 | | 1,153.0 | |
| Plaque burden, mm ³ | 304.61 | | 424.61 | | 496.73 | |
| | EEM | Lumen | EEM | Lumen | EEM | Lumen |
| Length, mm | 45.85 | 46.43 | 64.02 | 64.81 | 72.00 | 72.72 |
| Tortuosity ¹² | 0.12 | 0.13 | 0.15 | 0.16 | 0.15 | 0.16 |
| Mean radius, mm | 1.88 | 1.28 | 1.28 | 1.21 | 2.43 | 1.96 |
| Aspect ratio ¹³ | 24.39 | 36.27 | 35.43 | 53.39 | 29.65 | 37.19 |
| Curvature relationship, $\times 10^{-3}$ | 8.80 | 5.54 | 5.86 | 3.33 | 14.7 | 11.1 |
| Torsion value ¹² | 0.94 | 0.24 | 0.57 | 0.32 | 1.18 | 0.55 |
| Bending energy ¹⁴ | 4.48 | 5.31 | 7.94 | 9.32 | 10.61 | 11.66 |
| Torsion energy ¹⁴ | 334.4 | 229.50 | 779.5 | 759.46 | 1,103.13 | 870.65 |
| Mean curvature, mm ⁻¹ | 0.04 | 0.04 | 0.038 | 0.04 | 0.04 | 0.04 |
| Total curvature, mm ⁻¹ | 4.3 | 5.00 | 6 | 6.47 | 6.54 | 7.30 |
| Mean torsion, mm ⁻¹ | -0.15 | -0.14 | -0.1 | -0.04 | -0.17 | -0.16 |
| Total torsion mm ⁻¹ | 20.35 | 23.23 | 34.33 | 33.64 | 38.63 | 42.58 |
| Mean combined curvature, ¹³ mm ⁻¹ | 0.20 | 0.22 | 0.23 | 0.22 | 0.25 | 0.26 |
| Total combined curvature, ¹³ mm ⁻¹ | 22.03 | 24.78 | 36.43 | 36.21 | 40.94 | 45.01 |

EEM: external elastic membrane.

length, tortuosity, total bending, and twisting). The difference of these characteristics stemmed from lesions, but could also be related to the presence of branches (bifurcations).

Discussion

In comparison with other tests related to three-dimensional reconstruction such as CT, this model has some strengths: better spatial resolution of the lumen vessel, and greater accuracy in the delimitation of the vessel wall and in the details of the type of vascular remodeling. Unlike CT, which provides information of the entire coronary tree, reconstruction by IVUS-AX provides information about the study's target vessel. However, in the vessel in question, this model allows for visualization of coronary atherosclerotic disease in a more accurate way, through the precise location of the lesion and of plaque distribution. The synergistic integration of IVUS with AX allows for increasing the volumetric accuracy of the vessel lumen and the vascular wall, considering the curves and the spatial location of the vessel. This tool has the power to facilitate the recognition of characteristics of atherosclerotic disease, as exposed by IVUS (EEM data, remodeling, plaque burden, etc.), as well as detailing aspects insufficiently described by coronary angiotomography.

The geometric characterization of coronary arteries, as set out in this study, opens the door for future research and studies on the development and progression of atherosclerotic plaques. Due to the small diameter and movement of coronary arteries, it was not possible to directly measure the shear stress. In this context, the three-dimensional reconstruction is essential to calculate variables such as wall shear stress (WSS) or oscillatory shear index (OSI), by performing computational fluid dynamics simulations. Atherosclerotic plaques are related to shear stress, both as cause and as effect. In the development of atherosclerotic disease, positive remodeling prevents the growth of plaque into the vessel lumen. However, when the remodeling fails to offset this growth, the plaque will protrude into the vessel lumen by modifying the shear stress (cause and effect). The biological impact of changes in shear stress on plaque composition and on its vulnerability are not yet fully understood; nonetheless, it is known that the regions of the plaque subjected to high shear stress are more vulnerable and will have thinner and more fragile fibrous layers, predisposing to rupture. Therefore, a robust model of three-dimensional coronary reconstruction allows for the study of the relationship between shear stress, location, and plaque progression, as well as in-stent restenosis.

Moreover, through three-dimensional reconstructions, computational fluid dynamics can be applied to obtain local flow velocity and a functional evaluation of intermediate lesions, through numerical simulation of hemodynamic phenomena (virtual fractional flow reserve).

The classic technique of three-dimensional coronary reconstruction using a fusion of IVUS with biplane AX is known as ANGUS. The lumen contours and EEM are defined by IVUS, and the AX biplane data are used to determine the three-dimensional position of each IVUS frame. This procedure has been validated and is being used by several research groups, including for evaluation of shear stress in human coronary arteries. Compared to the ANGUS method, the method presented in this study exempts biplane AX, a technique not available in Brazilian hospitals. In addition, there was no need for online gating with electrocardiogram, which only retrieves a cardiac cycle phase.⁴ In fact, offline gating was applied based on image⁵ retrieval of 15-30 phases/study, allowing, in the future, four-dimensional reconstructions (space and time). Furthermore, this study used biplane snakes¹⁰ for the reconstruction of the catheter center line (core line) instead of the MacKay method.¹⁵ In this proposed alternative, the interaction with the operator consists of indicating the

beginning and end of the pullback (points clearly distinguishable in IVUS images), whereas in the McKay method, over six non-coplanar points should be provided for each of the two images, thus making the initialization a more complex task. Additionally, biplane snakes allow a simple extension to use non-orthogonal AXs.¹⁶

Conclusions

The methodology presented for vessel reconstruction allows for greater data extraction compared to the classical reconstruction by CT angiography, as well as an optimization of the reconstruction process, in relation to the ANGUS method. The synergistic integration between angiographic studies and intravascular ultrasound increases the volumetric accuracy of the vessel and the global visualization of the key aspects of the atherosclerotic disease, such as plaque remodeling and distribution.

Funding source

This research was supported by the following Brazilian agencies: Conselho Nacional de Desenvolvimento Científico e Tecnológico (CNPq), Fundação de Amparo à Pesquisa do Estado do Rio de Janeiro (FAPERJ), and Coordenação de Aperfeiçoamento de Pessoal de Nível Superior (CAPES) for the following centers: Laboratório Nacional de Ciências da Computação (LNCC) and Instituto Nacional de Ciências e Tecnologia em Medicina Assistida por Computação Científica (INCT/MACC).

Conflicts of interest

The authors declare no conflicts of interest.

References

1. Parker DL, Pope DL, Van Bree R, Marshall HW. Three-dimensional reconstruction of moving arterial beds from digital subtraction angiography. *Comput Biomed Res.* 1987;20(2):166-8.
2. Wahle A, Wellnhofer E, Mugaru I, Saner HU, Oswald H, Fleck E. Assessment of diffuse coronary artery disease by quantitative analysis of coronary morphology based upon 3-D reconstruction from biplane angiograms. *IEEE Trans Med Imaging.* 1995;14(2):230-41.
3. Krams R, Wentzel JJ, Oomen JA, Vinke R, Schuurbiens JC, de Feyter PJ, et al. Evaluation of endothelial shear stress and 3D geometry as factors determining the development of atherosclerosis and remodeling in human coronary arteries in vivo: combining 3D reconstruction from angiography and IVUS (ANGUS) with computational fluid dynamics. *Arterioscler Thromb Vasc Biol.* 1997;17(10):2061-5.
4. Bruining N, von Birgelen C, de Feyter PJ, Ligthart J, Li W, Serruys PW, et al. ECG-gated versus non gated three-dimensional intracoronary ultrasound analysis: implications for volumetric measurements. *Cathet Cardiovasc Diagn.* 1998;43(3):254-60.
5. Maso Talou G, Larrabide I, Blanco P, Bezerra C, Lemos P, Feijóo R. Improving Cardiac Phase Extraction in IVUS Studies by Integration of Gating Methods. *IEEE Trans Biomed Eng.* 2015 Jun 24. Epub ahead of print.
6. Krissian K, Westin CF, Kikinis R, Vosburgh KG. Oriented speckle reducing anisotropic diffusion. *IEEE Trans Image Process.* 2007;16(5):1412-24.
7. Maso Talou GD. Segmentação de imagens IVUS via contornos ativos e reconstrução espaço-temporal dos vasos coronários assistida por angiografias. *Dissertação de Mestrado.* Petrópolis, RJ: Laboratório Nacional de Ciências da Computação; 2013.
8. Kass M, Witkin A, Terzopoulos D. Snakes: Active contour models. *Int J Comput Math.* 1988;1(1):321-331.
9. Xu C, Prince JL. Snakes, shapes, and gradient vector flow. *IEEE Trans Image Process.* 1998;7(3):359-69.
10. Canero C, Radeva P, Toledo R, Villanueva J, Mauri J. 3D curve reconstruction by biplane snakes. In: *Proceeding IEEE of 15th International Conference on Pattern Recognition, ICPR'00.* Barcelona, Spain: IEEE Computer Society; September 3-8, 2000. v. 4. p. 563-6.
11. Antiga L, Ene-Iordache B, Remuzzi A. Computational geometry for patient-specific reconstruction and meshing of blood vessels from MR and CT angiography. *IEEE Trans Med Imaging.* 2003;22(5):674-84.

12. Bogunović H, Pozo JM, Cárdenes R, Villa-Uriol MC, Blanc R, Piotin M, et al. Automated landmarking and geometric characterization of the carotid siphon. *Med Image Anal.* 2012;16(4):889-903.
13. Mut F, Wright S, Ascoli GA, Cebal JR. Morphometric, geographic, and territorial characterization of brain arterial trees. *Int J Numer Method Biomed Eng.* 2014;30(7):755-66.
14. Meng S, Geyer SH, Costa Lda F, Viana MP, Weninger WJ. Objective characterization of the course of the parasellar internal carotid artery using mathematical tools. *Surg Radiol Anat.* 2008;30(6):519-26.
15. MacKay SA, Potel MJ, Rubin JM. Graphics methods for tracking three-dimensional heart wall motion. *Comput Biomed Res.* 1982;15(5):455-73.
16. Yang J, Cong W, Chen Y, Fan J, Liu Y, Wang Y. External force back-projective composition and globally deformable optimization for 3-D coronary artery reconstruction. *Phys Med Biol.* 2014;59(4):975-1003.